Aalborg Universitet

A New Position Detection and Status Monitoring System for Joint of SCARA

Lu, Wenqi; Tang, Bo; Wu, Yaxiong; Lu, Kaiyuan; Wang, Dong; Wang, Xiufeng

A New Position Detection and Status Monitoring System for Joint of SCARA

Wenqi Lu, *Member, IEEE*, Bo Tang, Yaxiong Wu, Kaiyuan Lu, *Member, IEEE*, Dong Wang, *Member, IEEE*, and Xiufeng Wang

Abstract—**High precision position detection of joint and status monitoring of speed reduction gearbox (SRG) are two key technologies in the research and development of selective compliant assembly robot arm (SCARA). The existing schemes have some problems, such as the large occupation of space, high cost, complex implementation, lack of status monitoring, etc. Therefore, firstly, in order to get the accurate position information of joint when the SCARA is powered up at the first time, a new combined incremental encoder with unevenly distributed multiple indexing signals and initial position detection method is proposed. Secondly, in order to get the accurate position information and monitor the operation status of the SRG during the positioning operation, a real-time position detection and status monitoring method based on the transmission error using dual incremental encoder is proposed. The general design principle has been given, and various experimental results have confirmed the effectiveness of the proposed solution. The proposed new combined incremental encoder has the advantage of small occupied space, easy realization and low cost. The proposed position detection and status monitoring method not only realizes the high precision detection of the joint position but also provides the key data for the monitoring of the running state of the SRG.**

Index Terms—**Selective compliance assembly robot arm, unevenly distributed multiple indexing signals, combined incremental encoder, dual incremental encoder, status monitoring.**

I. INTRODUCTION

WITH the continuing developments of industrial automation, the selective compliance assembly robot

arm (SCARA), due to its simple structure, high positioning accuracy, fast dynamic response features, has found many applications in the automatic assembly line, cargo transportation, PCB soldering, etc. [1-3].

The existing SCARA manipulator joint has two different design structures, depending on how the drive and control unit is placed concerning the servo motor and its drive train. In the first design structure, the motor (with an encoder), driver, encoder and SRG are designed independently and assembled as a whole to form a mechanical arm joint. Multiple joints need to be designed with multiple independent drives and main controllers to form an independent control cabinet, which is designed and installed separately from the manipulator body, as illustrated in Fig. 1[4]. This kind of design requires a large space typically for placing the SCARA, and the cost is also high. It is suitable for applications requiring high-performance trajectory control and typical products of this kind of SCARA are from YAMAHA, KUKA, etc. The other design architecture is to integrate the drive and encoder into the drive shaft of the servo motor, as illustrated in Fig. 2[5]. Often, a hollow shaft is used for this mechanically integrated design. And the main controller is placed in the base of the mechanical body without an independent control cabinet. This is a relatively low-cost solution, and typical products are from EPSON. It is suitable for applications with point control, such as moving and palletising. Among them, joint position detection with high-precision and high-response has become one of the critical technologies in the development of manipulators [6-7]. The SRG is an essential component in the drive trains of SCARA. SRG failures have caused significant downtime of SCARA and significant financial losses [8]. Thus, the fault monitoring of SRG is of great importance in the condition monitoring systems for SCARA.

For the detection of the position information, many methods have been proposed. In [9-10], the sensorless control technology is used to estimate the position information of the motor, which has been widely used in some speed regulation drive occasions. However, the accuracy of the position estimation depends on the motor parameters, and the dynamic response and reliability of the closed-loop system are weaker than that of the encoder system in the transient process. The current technical level can not meet the requirements of high-precision positioning of manipulator's joints.
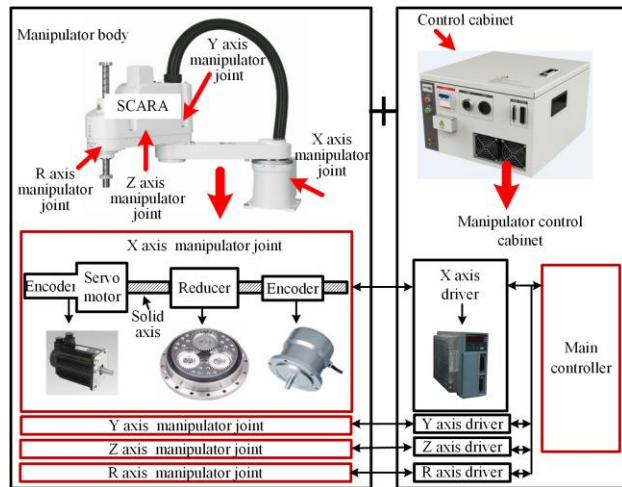
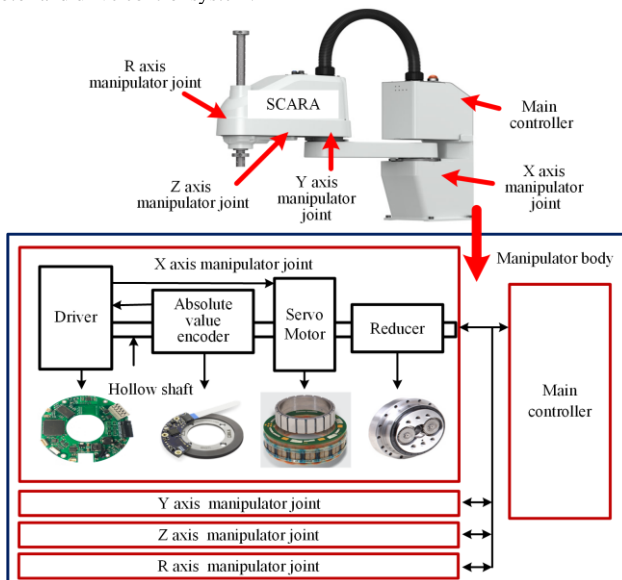Fig. 1. Schematic diagram of the four-axis SCARA scheme with independent motor and drive control system.

Fig. 2. Schematic diagram of the four-axis SCARA scheme with highly integrated motor and drive control system.

In [11-13], absolute photoelectric encoder and rotary transformer were used to provide the position information of the servo motor connected to the robotic arm. It can memorise the position of the joint during the initial power-on and the whole operation process, and can effectively obtain the initial position and real-time operation position information of the joint at any time. The position detection accuracy of the joint is closely related to the design accuracy of the absolute encoder. Higher the design accuracy of an absolute encoder is, better the precision of the position detection will be. But the design of disc for the absolute photoelectric encoder is complex, and the processing is difficult. The rotary transformer requires complex decoding circuits which require excessive hardware and signal processing efforts. It will increase the size and cost of the absolute encoder when compared to the incremental encoder for achieving the same position measurement accuracy. It is more suitable for a manipulator with large size, heavyweight and high cost, as shown in Fig. 1.

In [14-15], to reduce the cost, the absolute magnetic encoder is used to detect the position information. It can also obtain the real-time position information of the joint directly during the initial power-on and the whole operation process. Compared with the scheme designed by the absolute photoelectric encoder or rotary transformer, it has the advantage of simple structure and low cost on the design of the encoder body. However, the absolute magnetic encoder has high requirements for the design and assembly of hardware and software and support mechanism, and it is easy to introduce interference in the operation process, which will reduce the detection accuracy of the encoder. Moreover, as the main disadvantage for the absolute encoders (absolute photoelectric encoder, rotary transformer, absolute magnetic encoder, etc.), when these absolute encoders are used, special decoding circuits and batteries are needed which will also be limited by the joint space of the manipulator. It is not suitable for four-axis SCARA manipulator with small size and lightweight, as shown in Fig. 2.

In [16-18], an incremental encoder combined with Hall sensors separately mounted by 120 degrees were used to detect the position information. In the whole operation process, the real-time running position of the joint is detected and fed back by the incremental encoder. And the accuracy of real-time joint position detection is related to the number of incremental encoder lines designed. The higher the number of lines is, the higher the accuracy and cost of position detection will be. But compare to absolute encoders, the design of disc for the incremental encoder is simple, and the processing is easy, it does not need special decoding circuits and batteries. Thus, the size and cost of the incremental encoder are smaller when compared to the absolute encoder for achieving the same position measurement accuracy. However, the incremental encoder cannot memorise and provide the initial position of the joint when the power is on at the first time. In [16-18], the Hall sensors with an electric angle of 120 degrees apart are used to provide the initial position information. After the initial position is judged, the Hall sensor immediately stops working and switches to the incremental encoder. The hall sensor is a very low-cost solution, but its position detection error is large, which could reach 30 degrees. It is not suitable to start directly on the joint of the manipulator with a large inertia load. Moreover, the Hall sensor is also fragile, which limits the application areas of the SCARA.

For the status monitoring of the SRG, many methods [19-21] have also been proposed. Reference [19] proposes a novel dual-ELM network for fault diagnosis with an application to a multistage gearbox. Experimental results verify the effectiveness of the proposed method. Reference [20] proposes a multiscale filtering reconstruction method for the fault diagnosis of wind turbine gearbox under varying-speed and noisy conditions. The experimental results verify the effectiveness and superiority of the method, which has a good application prospect in the online fault diagnosis of the gearbox of the wind turbine in the environment of variable speed and noise. However, the above methods need to be equipped with auxiliary sensors and corresponding software and hardware to collect relevant information (such as vibration) in real-time, which will be limited by the cost and space in the practical application of manipulator.

The SCARA studied in this paper is mainly used for point position control, which is more suitable for the high integrated scheme shown in Fig. 2. However, in order to obtain the initial position of the mechanical arm joint when first powering on, the existing SCARA uses an absolute encoder. According to the previous analysis, the absolute encoder has the problems of large space occupation and high cost. Besides, the existing SCARA has no function of monitoring the running state of the reducer, and the method of installing auxiliary sensors and hardware circuits will also be limited by the space and cost of the manipulator under investigation.

Therefore, in order to further reduce the space and cost of the mechanical arm, and monitor the operation state of the reducer, considering that the initial position of the mechanical arm only needs to be obtained when it is powered on for the first time, a new combined incremental encoder with unevenly distributed multiple indexing signals and initial position detection method is proposed in this paper. Secondly, in order to get the accurate position information and monitor the operation status of the SRG during the positioning operation of SCARA, a real-time position detection and status monitoring method based on the transmission error using dual incremental encoder is proposed. In this paper, the design principle is described, the prototype of the manipulator is developed, and the algorithm is tested.

II. THE PROPOSED NEW POSITION DETECTION AND STATUS MONITORING SYSTEM OF SCARA JOINT

The principle and structure diagram of the x-axis manipulator joint of SCARA designed based on the proposed new position detection and status monitoring system is shown in Fig.3. It consists of an input encoder, a driver, an output encoder, a brake, a permanent magnet synchronous motor (PMSM), a speed reduction gearbox (SRG) and main controller, etc. A common incremental encoder is installed at the input end of the SRG as an input encoder and used for detecting the position information of the input end of the SRG. The driver controls the PMSM. An SRG is connected to the shaft of the PMSM, to meet the low-speed motion requirement of the robotic arm. In order to get the accurate position information of joint when the SCARA is powered up at the first time, a new combined incremental encoder with unevenly distributed multiple indexing signals is proposed as the output encoder, which is also installed at the input end of the SRG but used for detecting the position information of the output end of the SRG. This new encoder is connected with the output end through the hollow part of the SRG. When the motor is running, the position information of the output end is read at the input end of the SRG. And it is a low-cost and compact solution compared to traditional absolute encoders; it can detect the initial position by unevenly distributed index signals combined with simple control routines. Based on the proposed new encoder, a corresponding initial position detection method is proposed for the driver, and during the positioning operation of SCARA, to get the accurate position information and monitor the operation status of the SRG, a real-time position detection and status monitoring method based on the transmission error using the dual incremental encoder (common incremental and combined
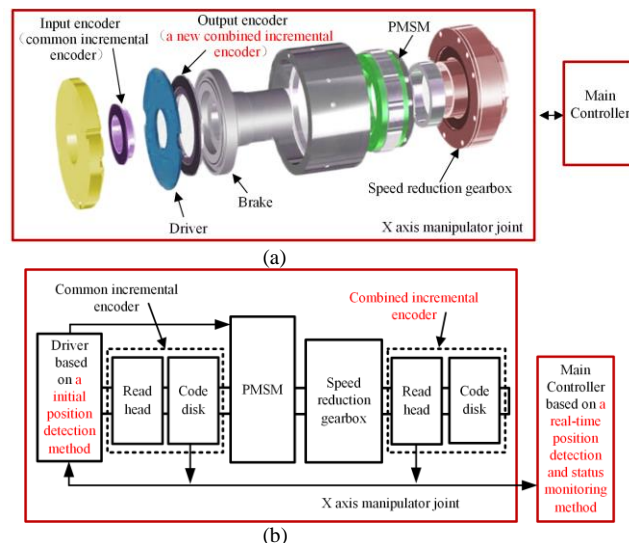

Fig.3. Principle and structure diagram of the x-axis manipulator joint. (a) structure diagram, and (b) principle diagram.
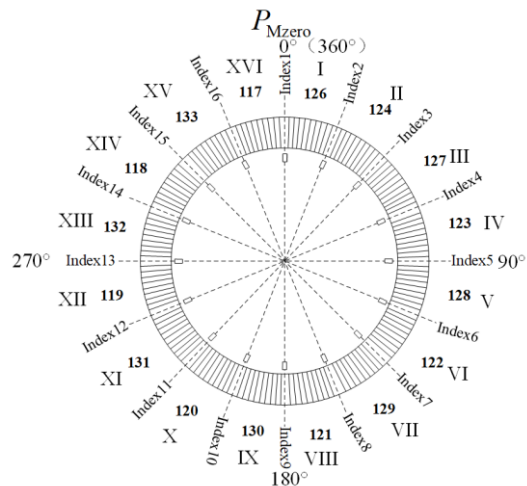
Fig. 4. Layout for code disk of the proposed combined encoder.

incremental encoder) is proposed for the main controller. The following is the elaboration of its content.

A. The proposed new combined incremental encoder

The proposed new combined incremental encoder is shown in Fig. 4. It may be observed that in addition to the traditional opaque and transparent sectors coded into the disk for providing incremental position change signals, 16 indexing signals (labelled from index1 to index 16) are added. Index signal is also often used in traditional incremental encoders. It normally generates a single pulse per revolution only, which is used for precise determination of a reference position. To use this index signal for absolute position detection or correction, it may require rotating the arm for 360 mechanical degrees to reach the index position. Using only one index signal for absolute position detection is also less fault-tolerant. Simply increasing the number of index signals cannot solve this problem, since different index signals generate the same pulse that cannot be distinguished by the controller.

In this new encoder design, as shown in Fig. 4, these 16 index signals are unevenly distributed on the disk, dividing the

360 degrees region into 16 different index sectors (labelled from I to XVI as indicated in Fig. 4). The absolute positions that different index signals corresponding to are listed in Table I. The design principle of these index sectors/signals is discussed below.

Supposing, the encoder generates 2000 pulses per 360 degrees (e.g. 2000 opaque and transparent sectors in the outer ring of the encoder, as shown in Fig. 4.). Dividing 360 degrees into 16 index sectors will naturally give 125 pulses per sector. To enable an uneven distribution, two neighbouring sectors are grouped, giving eight groups in total. The number of pulses of the first sector in the first group is increased by 1 (giving 126 pulses) and the number of pulses of the second sector in this first group is reduced by 1 (giving 124 pulses). Repeat this procedure for the second group but by increasing/decreasing the number of pulses for the first and second sectors by 2, respectively. Following this pattern, each index sector will then have its unique number of pulses, as listed in Table I. Each sector is bounded by two index signals. Their corresponding positions are given in Table II as well, assuming an anti-clockwise rotational direction travelling from the 'FirstIndex' boundary position to the 'SecondIndex' boundary position (Table II).

Following the design routine mentioned above, it may be generalized that the number of pulses (ΔL) contained in the ith sector (ΔL_i) may be expressed as:

$$\Delta L_{i-1} = L_{ls}/M + i/2 \qquad (1)$$

$$\Delta L_i = L_{ls}/M - i/2 \qquad (2)$$

where, L_{ls} is the number of pulses (lines) per revolution for this combined encoder located at the low-speed side of the gearbox; M is the total number of sectors separated by the index signals and $i = 2,4,6,... <= M$. In the case study mentioned above, $L_{ls} = 2000$ and $M = 16$.

By adding the number of pulses per individual sector starting from sector I, it is not difficult to find the absolute position of each index signal that corresponds to, as

$$\theta_{idx,j} = (j-1)\frac{L_{ls}}{M} \times \frac{360°}{L_{ls}} = (j-1)\frac{360°}{M}, \quad j = 1,3,5,... \qquad (3)$$

and

$$\theta_{idx,j} = \left[(j-1)\frac{L_{ls}}{M} + \frac{j}{2}\right] \times \frac{360°}{L_{ls}}$$
$$= (j-1)\frac{360°}{M} + j\frac{180°}{L_{ls}}, \quad j = 2,4,6,... \qquad (4)$$

B. The proposed Initial position detection by using the proposed combined incremental encoder

Based on the proposed new combined incremental encoder, a corresponding initial position detection method is proposed, as shown in Fig. 5. Suppose initially, and the robotic arm is parked at a position indicated by P_{ini}, which is located in sector III, as shown in Fig. 5(b). To detect this initial position, the arm is first driven to rotate in a clockwise direction until it reaches the first index position ('Index4' for this case). The number of pulses

TABLE I
THE ANGLE VALUE OF THE CODE DISK AT DIFFERENT INDICES

Symbol	Encoder angle (degrees)	Index	Encoder angle (degrees)
Index1	0	Index9	180
Index2	22.68	Index10	203.4
Index3	45	Index11	225
Index4	67.86	Index12	248.58
Index5	90	Index13	270
Index6	113.04	Index14	293.76
Index7	135	Index15	315
Index8	158.22	Index16	338.94

TABLE II
THE ANGLE VALUE OF THE CODE DISK AT THE LOCATION OF THE TWO INDEXES WITH DIFFERENT PULSE DIFFERENCE

Pulse difference of combined encoder (ΔL)	Pulse difference of absolute encoder (ΔL)	The encoder angle at FirstIndex ($\theta_{FirstIndex}$) (degrees)	The encoder angle at SecondIndex ($\theta_{SecondIndex}$) (degrees)
126	11340	22.68	0
124	11160	45	22.68
127	11430	67.86	45
123	11070	90	67.86
128	11520	113.04	90
122	10980	135	113.04
129	11610	158.22	135
121	10890	180	158.22
130	11700	203.4	180
120	10800	225	203.4
131	11790	248.58	225
119	10710	270	248.58
132	11880	293.76	270
118	10620	315	293.76
133	11970	338.94	315
117	10530	0	338.94

generated by this rotation will be recorded, and the angle between the initial parking position and the position marked by 'Index4' can be known (denoted as θ_{IF}). Then, starting from the 'Index4' position, the arm is driven to rotate in an anti-clockwise direction until it reaches the second index position – this will be 'Index3' position in this case study. The generated number of pulses (denoted as ΔL) rotated from 'Index4' to 'Index3' will be 127, and this number is unique. By using Table II, the sector number can be identified, the relative position corresponding to the second index position aligned with 'Index3' (denoted as current position $\theta_{SecondIndex}$) and the relative position corresponding to the first index position aligned with 'Index4' (denoted as $\theta_{FirstIndex}$) are then identified. The initial position can be calculated from $\theta_{FirstIndex}$ and θ_{IF}. The angle (denoted as θ_{cur}) between this current position and the desired mechanical zero position is also found. The arm may then be rotated back to the mechanical zero position indicated as P_{Mzero} in Fig. 5, is ready for the following required operations. Based on the previous analysis, because of the existence of the speed reducer (with a gear ratio of 80), when the encoder on the low-speed side generates a pulse, the encoder on the high-speed side will generate 80 pulses if there is no transmission error. The initial position and current position of the manipulator's joint can be calculated according to (5) and (6).
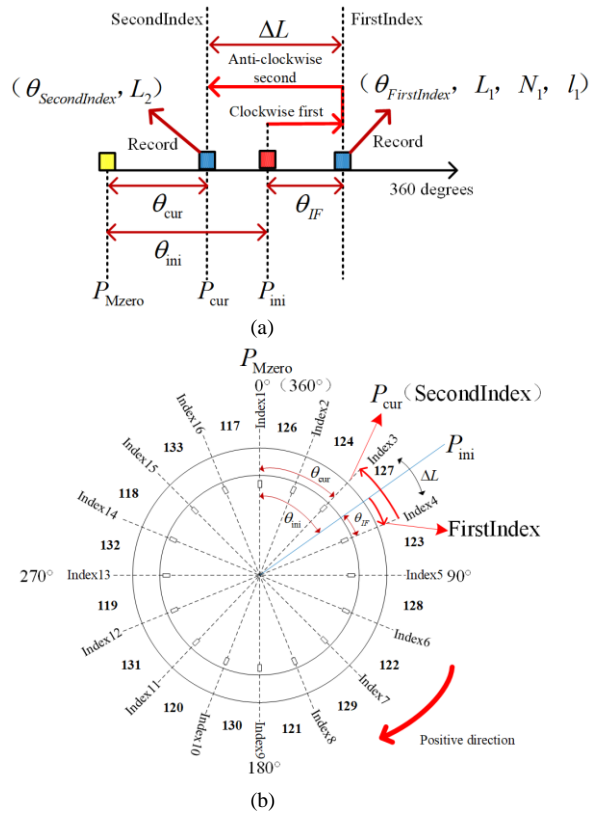
Fig. 5. Schematic diagram of the initial position detection method. (a) detection principle, and (b) an example of the working principle demonstration.
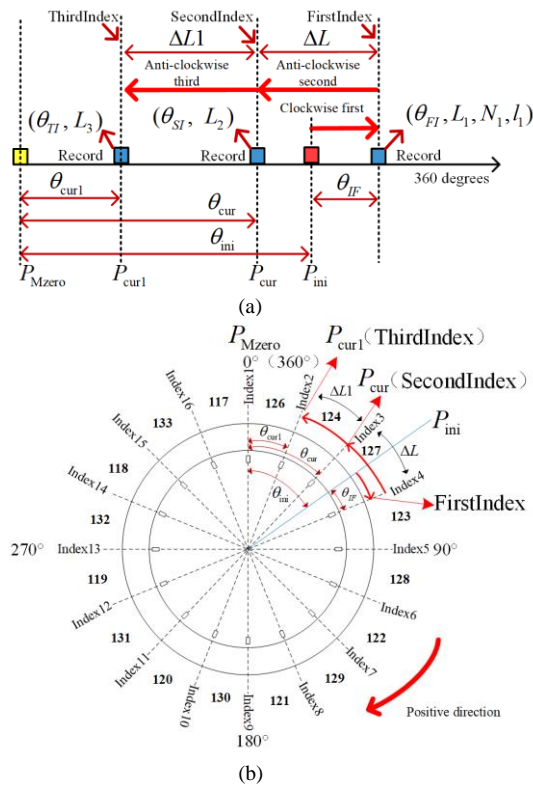

Fig. 6. Schematic diagram of the enhanced initial detection method. (a) detection principle, and (b) an example of the working principle demonstration.

$$\theta_{ini} = \theta_{FirstIndex} - \Delta L_{hs} \times 360 / (k_{gear} L_{hs}) \qquad (5)$$

$$\theta_{cur} = \theta_{SecondIndex} \qquad (6)$$

where, ΔL_{hs} is the number of pulses fed back by the high-speed encoder, during the rotation from the original parking position to the first index position, k_{gear} is the reduction ratio, L_{hs} is the number of pulses (lines) per revolution for common encoder located at the high-speed side of the gearbox.

In addition, considering the distortion of code disk, incorrect installation of components, or the introduction of interference may cause the loss of the pulse difference between the two indexes, in order to further improve the robustness and reliability of the initial position detection method, two solution methods are proposed as follows: firstly, improve the processing technology, installation specifications and anti-interference measures, so as to ensure the detection accuracy on the hardware side; secondly, according to the allowable swing range of the mechanical arm during power on, on the basis of the obtained two indexes for each forward rotation and reversed rotation as shown in Fig. 5, an enhanced detection method is proposed for the initial position detection by introducing one more reversed rotation, and the corresponding index and pulse error calculation method is shown in Fig. 6, which is integrated into the developed mechanical arm products, as a redundant scheme.

C. The proposed real-time position detection of positioning and status monitoring method based on the transmission error

It is known from the reference [22-24] that there are machining errors and unstable errors in the actual operation of the SRG. The machining errors mainly include manufacturing errors and assembly errors, which are often caused by human or environmental factors. The unstable error mainly comes from three aspects: during the actual operation of the transmission chain, due to the direct effect of the load and the dynamic meshing force generated at high speed, the components are elastically deformed; Under the continuous high-speed operation, the temperature of the contact position of the component rises, which leads to its thermal deformation; after a long time of operation, components wear, resulting in system instability. These errors are generated in the actual operation of the component and change with the operation state. Therefore, there must be a minimum transmission error (called allowable error in this paper) in the normal operation of the SRG itself without fault. Considering the backlash of reducer, the minimum transmission error is closely related to the backlash and the reduction ratio. The greater the backlash is, the greater the minimum transmission error will be. But when the reducer is running normally, its maximum clearance will not exceed the product specifications. When the SRG fails, it is also known from [22-24] that the transmission error of the SRG will increase with the occurrence of the gearbox fault (mainly gear fault and rolling bearing fault), thus exceeding the allowable error. In this paper, the two encoders are installed on both ends of the SRG, and the transmission error can be easily obtained by using the data of the two encoders as (7), which provides a simple and effective method for online detecting the potential fault of the gearbox. Therefore, a real-time position detection and status monitoring method is proposed based on the

transmission error using the dual incremental encoder. Compared with the traditional method [24-25], this method does not need additional sensors and supporting hardware and software systems.

$$\Delta P = P_{out}L_{hs}k_{gear}\big/L_{ls} - P_{in} + P_{backlash}L_{hs}k_{gear}\big/(3600\times360) \qquad (7)$$

where, $P_{backlash}$ is the backlash of reducer, which is 10arcsec according to the appendix, P_{in} is the number of pulses obtained by the encoder at the high-speed side of the gearbox, P_{out} is the number of pulses obtained by the encoder at the low-speed side of the gearbox, ΔP is the transmission error.

III. EXPERIMENTAL VALIDATIONS

A. Experiment platform design

The key components and whole machine of the four-axis SCARA based on the proposed methods are designed, as shown in Fig. 7. It consists of four drive unit, as principally described in Fig. 2. The proposed combined incremental encoder is shown in Fig.7(a), where the 16 unevenly distributed indexing markers can be observed when comparing to the standard incremental encoder, as shown in Fig. 7(b). The encoder reader, harmonic reducer and its drive unit are shown in Fig. 7(c), Fig. 7(e) and Fig. 7(d), respectively. As mentioned before, a hollow shaft is adopted for the integrated design of this SCARA.

In order to verify the correctness of the proposed combined encoder and the proposed initial position detection method, a test platform is designed, as shown in Fig. 8 (a) and (b), which consists of an absolute encoder (resolution ratio is 180000), the proposed combined encoder, a permanent magnet synchronous motor, a servo driver, a data acquisition card, and a microcomputer, etc. The motor is driven by a servo driver. The

absolute encoder and the proposed combined encoder are installed on the output shaft of the same motor. The pulse number of the two encoders is fed back to the computer through the data acquisition card for calculation and comparison. Because the absolute encoder can detect the initial position directly when it is powered on, the combined encoder first performs zero calibration with the absolute encoder when it is installed, and then the performance comparison test is carried out according to the initial position detection method as shown in Fig. 5. For verifying the effectiveness of the combined encoder, this paper has designed a real prototype of the robotic arm (as shown in Fig. 8(c)). The robotic arm has an integrated joint module shown in Fig. 3, as discussed before.

(a)

(b)

(c)
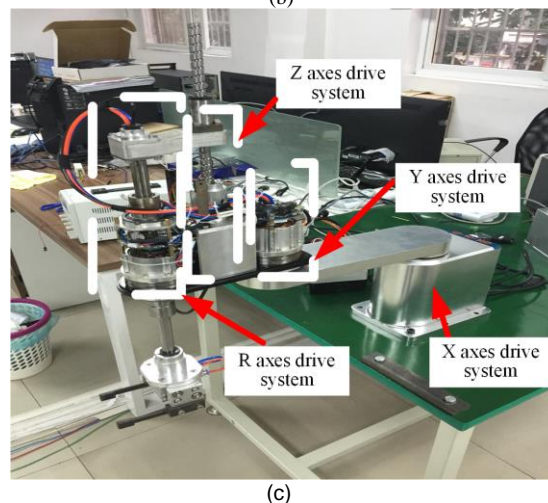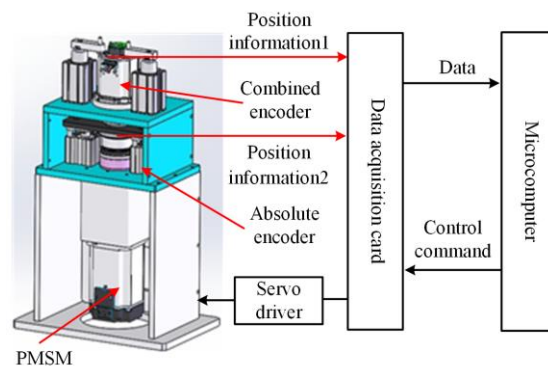
Fig. 8. The encoder comparison test platform and the whole machine of SCARA. (a) schematic diagram of encoder comparison test platform, (b) the encoder performance comparison test platform, and (c) whole machine.
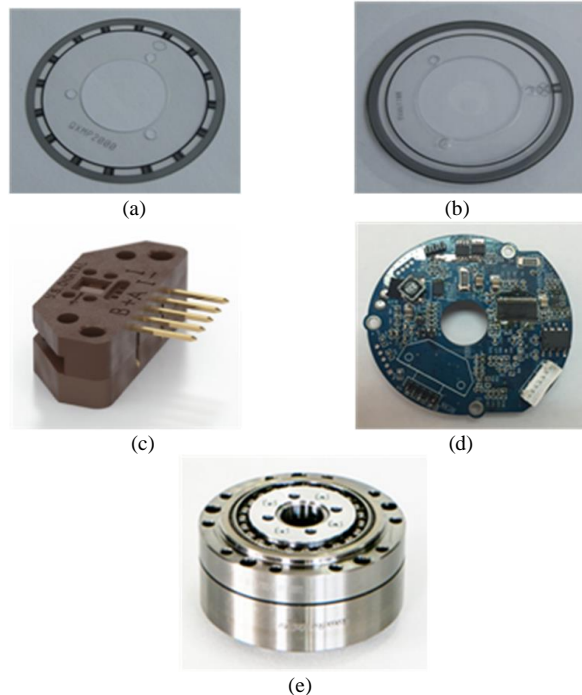

Fig. 7. The key components of the SCARA. (a) code disk of the proposed combined encoder, (b) code disk of a common incremental encoder, (c) read head for the code disk, (d) driver integrated with a read-head, and (e) harmonic reducer.

TABLE III
THE COMPARISON BETWEEN THE ABSOLUTE ENCODER AND COMBINED ENCODER

	Absolute encoder	Combined encoder
Cost (dollar)	About 72	About 29
Code disc diameter (inside/outside)(mm)	83/115	45/67
Weight (kg)	0.4	0.1

B. Performance test of the combined encoder

In order to verify the correctness of the proposed combined encoder and the proposed initial position detection method, a performance comparison test is taken based on the test platform, as shown in Fig. 8(a) and Fig. 8(b). And the cost, size and weight of the encoder are compared, as shown in Table III. It can be seen from the data that the cost, size and weight of the proposed combined encoder are better than that of the absolute encoder.

Firstly, the motor is manually adjusted to the mechanical zero position. Based on this, the initial position detection test is performed. The experimental waveform is obtained, as shown in Fig. 9. It can be seen from the waveform that the initial position of the motor can be obtained as soon as the power is turned on from the absolute encoder, but it cannot be obtained with the combined encoder proposed in this paper. The initial position detection performance test of the motor is carried out by the method shown in Fig. 5, and the waveform of Fig. 9 is observed. In the first step, the motor runs in the positive rotational direction. When the first index is obtained, the number of pulses fed back by the absolute encoder and combined encoder is 11348 and 126, respectively. In the second step, the motor runs in the reversed direction. When the second index is obtained, the number of pulses fed back by the absolute encoder and combined encoder is 5 and 0, respectively. Using the data in Tables I and II in the paper, we can see that the initial position obtained by the absolute encoder is 0.000 degrees while the current position is 0.010 degrees. The initial position obtained by the combined encoder is 0.00 degrees, while the current position is 0.00 degrees. The position accuracy of the two encoders is different, the error of absolute value encoder is smaller, which is 0.000 degrees, while the error of the combined encoder is relatively larger, which is 0.010 degrees. This error is related to the number of scale lines of the code disk. The feasibility of the proposed initial position detection method is validated. If higher accuracy is needed, more scale lines should be used. For the current application, the position error of 0.010 degrees is acceptable.

Secondly, the motor is manually adjusted to an arbitrary position, and the initial position detection test is performed. The experimental waveform is shown in Fig. 10. It can be seen from the waveform that the initial position of the motor can be obtained as soon as the power is turned on with absolute encoder, which is 80.484 degrees but cannot be obtained with the combined encoder. The initial position detection performance test of the motor is carried out by the method shown in Fig. 5, and the waveform of Fig. 10 is observed. In the first step, the motor runs in the positive rotational direction. When the first index is obtained, the number of pulses fed back by the absolute encoder and combined encoder is 45018 and 53, respectively. In the second step, the motor runs in a reversed
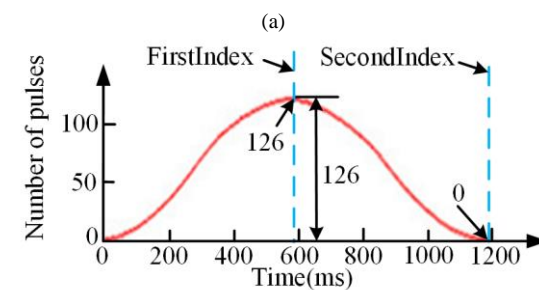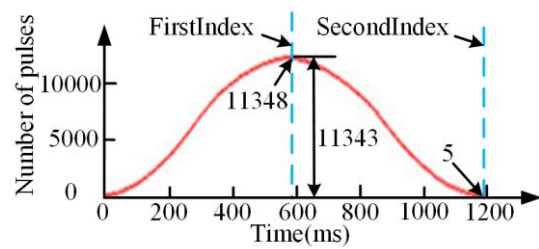

(a)

(b)

Fig. 9 Test of the initial position detection with two encoders at zero position. (a) absolute encoder, and (b) combined encoder.
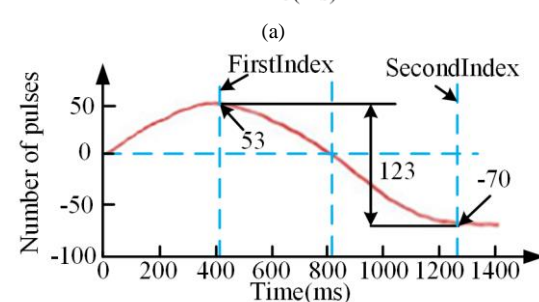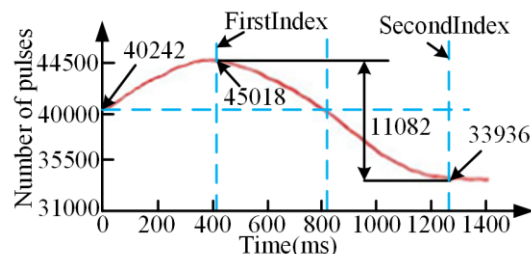

(a)

(b)

Fig.10 Test of the initial position detection with two encoders at an arbitrary position. (a) absolute encoder, and (b) combined encoder.

direction. When the second index is obtained, the number of pulses fed back by the absolute encoder and combined encoder is 333936 and -70, respectively. Using the data in Tables I and II in the paper, we can see that the initial position obtained by the absolute encoder is 80.484 degrees while the current position is 67.872 degrees. The initial position obtained by the combined encoder is 80.46 degrees, while the current position is 67.86 degrees. The error of absolute value encoder is smaller, which is 0.000 degrees. In comparison, the error of the combined encoder is larger, which is 0.024 degrees. For the current application, the position error below 0.1 degrees is already good enough.

Therefore, according to the above test waveforms, the combined encoder and the initial position detection method proposed in this paper can accurately and reliably obtain the initial position and current position information of the motor.

Based on the obtained current position information, the mechanical zeroing or positioning operation can be then carried out.

C. Transmission error analysis of SRG

According to formula (7), the transmission error curve of the SRG used in this paper can be obtained when it operates in the normal working range, as shown in Fig. 11. According to the observation waveform, although the SRG has entered a stable operation state, its transmission error still changes periodically in a small range, and the maximum transmission error (allowable error) is ±82 pulses. In the actual working process, when the transmission error exceeds the allowable error, the fault is considered to occur.

D. Performance test of the initial position detection

The validation of the initial position detection of the robotic arm by using the proposed combined incremental encoder is demonstrated by two case studies given below.

First, the robotic arm is pre-set to 36 degrees. According to Fig. 4, this position is bounded by Index2 and Index3, as described in section II. To detect the initial position, the arm is first rotated along the clockwise direction; 50 pulses are detected before detecting an index signal as indicated in Fig. 12(a). Then the arm is controlled to rotate along the anti-clockwise direction, 124 pulses are detected before another index signal is detected. Then according to Table II and Fig. 4, the initial parking position of the arm is located in zone II; when arriving at the first index position (Index3), the corresponding absolute position is $\theta_{FirstIndex} = 45$ degrees and when arriving at the second index position (Index2), $\theta_{SecondIndex} = 22.68$ degrees. During the rotation from the original parking position to the first index position, the low-speed side combined encoder generates 50 pulses while the high-speed side encoder indicates two complete revolutions (i.e. $\Delta L_{hs} = 4000$ pulses). Knowing the gear ratio is $k_{gear} = 80$, the initial parking position can be determined to be 36 degrees according to (5).

As another case study, the initial position is pre-set at 45 degrees. A similar procedure is repeated, and the obtained results are shown in Fig. 13. It may be observed that during the first clockwise rotation, 127 pulses are detected before reaching the first index position; the number of pulses generated is 127 during the anti-clockwise rotation from the first index position to the second index position. According to Table II and Fig. 4, the initial parking position is found to be located in sector III, and the corresponding boundary index signal positions are $\theta_{FirstIndex} = 67.86$ degrees and $\theta_{SecondIndex} = 45$ degrees, respectively. During the rotation from the initial parking position to the first index position, the high-speed side encoder generates a total of 10160 pulses. Then similar according to (5), the initial position can be found to be 45 degrees.

Therefore, the above experimental results prove that the initial position detection method proposed in this paper is effective. Limited to the space of this paper, the experiment of
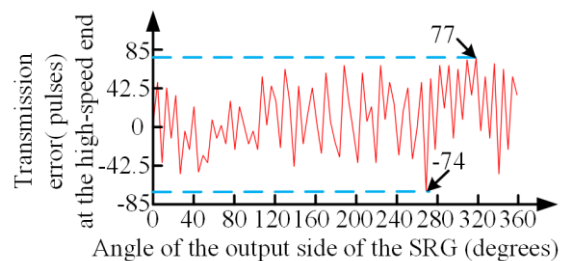

Fig. 11. Transmission error of the SRG itself (pulses number difference at the high-speed end).
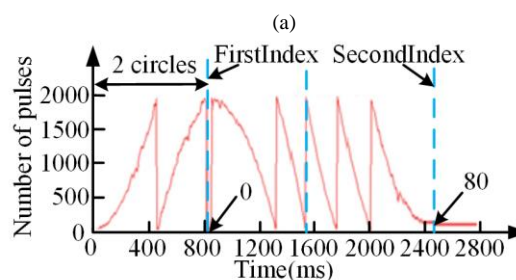

(a)

(b)
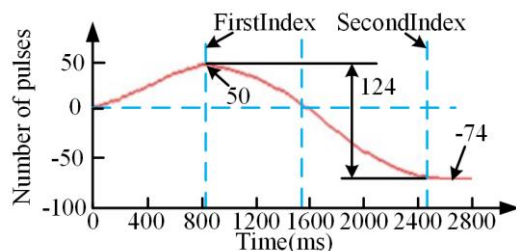
Fig. 12. Initial position detection test when setting the initial position at 36 degrees. (a) pulse number of the proposed combined encoder feedback, and (b) pulse number of the high-speed side incremental encoder feedback.

(a)

(b)

Fig. 13. Initial position detection test when setting the initial position at 45 degrees. (a) pulse number of the proposed combined encoder feedback, and (b) pulse number of the high-speed side incremental encoder feedback.
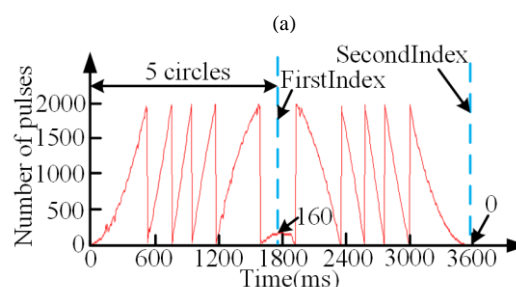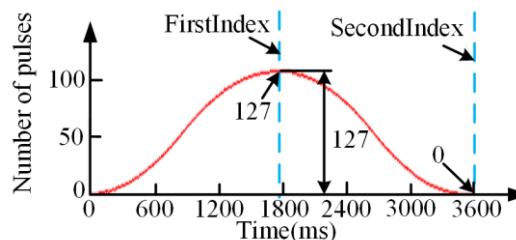
enhanced initial position detection method is not given. But according to the above experimental results, the proposed enhanced initial position detection method proposed in this paper is already very effective.
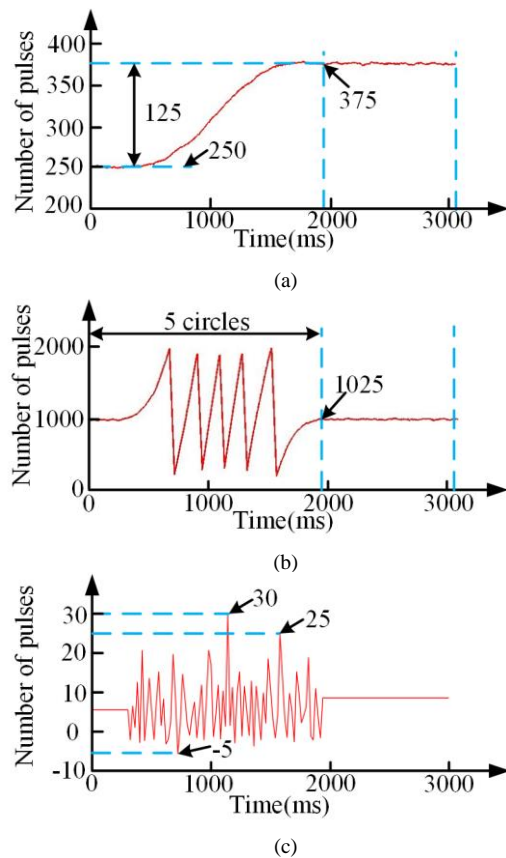
(a)

(b)

(c)

Fig. 14. Real-time position detection test when the positioning operation angle is 22.55 degrees. (a) pulse number of the proposed combined encoder feedback, (b) pulse number of the high-speed side incremental encoder feedback, and (c) pulse number difference at the high-speed end.

(a)

(b)

(c)

Fig. 15. Real-time position detection test when the positioning operation angle is 45.05 degrees. (a) pulse number of the proposed combined encoder feedback, (b) pulse number of the high-speed side incremental encoder feedback, and (c) pulse number difference at the high-speed end.

E. Position detection and status monitoring based on the transmission error during the positioning operation

In this experiment, firstly, the SRG is let work normally. The robotic arm is parked at 45 degrees (measured at the gearbox low-speed end), and the operation command is set to rotate the arm along the positive direction by 22.55 degrees. Under this condition, the generated pulses of the low-speed side combined encoder are shown in Fig. 14(a) and the pulses generated by the high-speed side encoder is given in Fig. 14(b). The difference between the number of pulses generated by the two encoders when counted at the high-speed side is shown in Fig. 14(c).

It may be observed from Fig. 14(a) that for a rotational angle of 22.55 degrees, the combined encoder can produce 125 pulses only, which corresponds to a position change of $125/2000 \times 360 = 22.5$ degrees. If the combined encoder is used for providing the position information, the position detection error is 0.05 degrees. In the same operation, we can see from Fig. 14(b), the incremental pulses of the high-speed side encoder are counted to be 5 cycles plus 25 pulses. Considering that the gear ratio is 80, this corresponds to a position change of $(5 \times 2000 + 25)/2000 \times 360/80 = 22.556$ degrees at the low-speed (combined encoder) side. The position detection error is reduced to 0.006 degrees, which gives a smaller angular position detection error (improved by 88%) as expected. During this rotation, the maximum difference is 30 pulses, as indicated in Fig. 14(c), which is within the range of ±82 pulses.
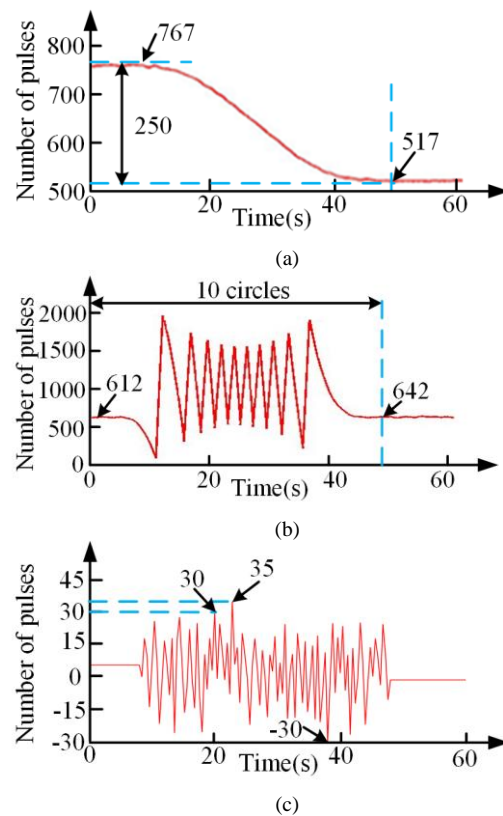
Another experiment is carried out when the operation command is set to rotate the arm in a negative direction by 45.05 degrees. Similar encoder pulses are recorded and shown in Fig. 15. It may be observed from Fig. 15(a) that the low-speed end encoder produces 250 pulses, indicating 45 degrees position change; while the high-speed side encoder produces in total 20030 pulses giving 45.0675 degrees. At the end of the positioning period, the position error is 0.05 degrees provided by the combined encoder alone; but the position error is reduced to 0.0175 degrees when the high-speed side encoder is used for position detection, which gives a smaller angular position detection error (improved by 65%) as expected. The difference of the number of pulses counted at the high-speed end of those two encoders shows a maximum of 35 pulses difference, which is within the range of ±82 pulses similar to the positive rotation situation. Therefore, it can be seen from the test results that when the SRG operates normally, the double encoder can accurately detect the joint position information and transmission error of the mechanical arm during the positioning process, and the transmission error of the SRG is within the allowable error.

Secondly, in case of failure of the SRG, in order to verify the effectiveness of the operation condition monitoring method, the SRG was disassembled, one of the gears was wear and tear, and the mechanical arm joint was reassembled. And the experiment is carried out when the operation command is set to rotate the arm in a positive direction by 22.50 degrees. Similar encoder pulses are recorded and shown in Fig. 16. During the forward operation, it may be observed from Fig.16(a) that the low-speed
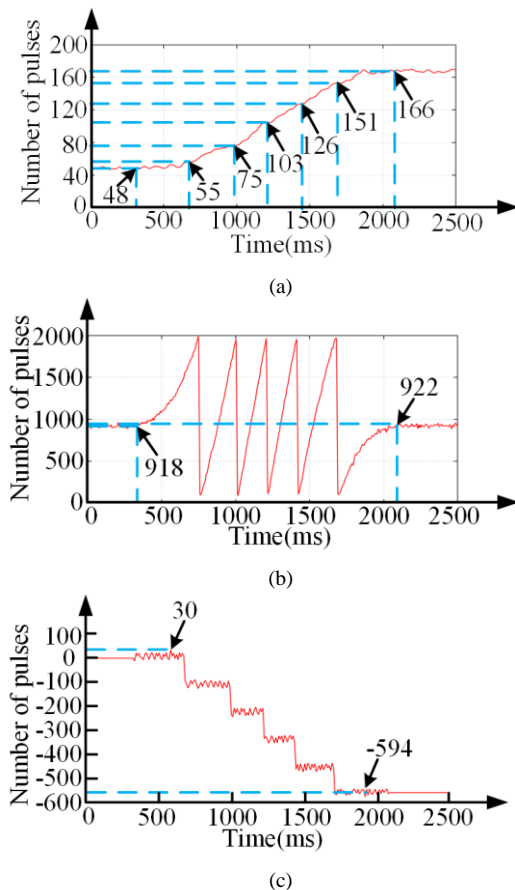
Fig. 16. Real-time position detection test when the positioning operation angle is 22.50 degrees. (a) pulse number of the proposed combined encoder feedback, (b) pulse number of the high-speed side incremental encoder feedback, and (c) pulse number difference at the high-speed end.

end encoder produces 118 pulses, indicating 21.24 degrees position change, while converting the 118 pulses to the high-speed end, it gives $118 \times 80 = 9440$ pulses; while the high-speed side encoder produces in total 10004 pulses giving 22.509 degrees, as shown in Fig. 16(b). The transmission error is -564 pulses, as indicated in Fig. 16(c), which exceeds the allowable error of the SRG at this time.

Therefore, in case of gearbox failure, the proposed method can realise fault detection and provide a method for online real-time detection of SRG operation state, which not only improves the safety factor of the manipulator but also provides key data and method for gearbox service life prediction [24-25].

IV. CONCLUSION

In order to obtain the initial position information of the joint accurately when the SCARA is powered on at the first time, a new combined incremental encoder with unevenly distributed multiple indexing signals and an associated initial position detection method are proposed, which has advantages of small space occupation, easy implementation and low cost, when compared with the existing encoder solutions. In order to obtain the real-time position information of the joint accurately and monitor the running state of the SRG in real-time in the process of SCARA positioning, a real-time position detection and status

monitoring method based on the transmission error using dual incremental encoder is proposed. In order to verify the correctness of the proposed combined encoder and the proposed initial position detection method, an encoder comparison test platform using an absolute encoder is designed, and the performance of the proposed combined encoder solution is validated. Taking a four-axis SCARA manipulator as the application object, the motor, dual encoders, actuators and other key components of the four joints were designed and tested. The results show that the initial position and the current position of the joint can be accurately detected using the proposed new combined incremental encoder and the associated initial position detection method. And the proposed encoder has advantages of simple structure, easy realization and low cost. The real-time position detection of the manipulator joint and monitor of the running state of the SRG can be achieved by the proposed method with high precision. The real-time monitoring of transmission error not only improves the safety factor of the manipulator but also provides the key data and methods for the service life prediction of the SRG. The SCARA designed based on the drive system not only has the advantages of small size, lightweight and high positioning accuracy but also has the function of SRG condition monitoring, which has already used in industrial application.

APPENDIX

Main parameters of joint of manipulator	
The line number of common Encoder	2000
The line number of combined Encoder	2000
Backlash of SRG	10arcsec
The gear ratio of SRG	1:80
Bodyweight	15kg

REFERENCES

[1] G. Oriolo, M. Cefalo and M. Vendittelli, "Repeatable Motion Planning for Redundant Robots Over Cyclic Tasks," *IEEE Transactions on Robotics*, vol. 33, no. 5, pp. 1170-1183, Oct. 2017.

[2] X. Li and C. C. Cheah, "Adaptive Neural Network Control of Robot Based on a Unified Objective Bound," *IEEE Transactions on Control Systems Technology*, vol. 22, no. 3, pp. 1032-1043, May. 2014.

[3] J. J. Craig, *Introduction to Robotics: Mechanics and Control*, 3rd ed. Upper Saddle River, NJ, USA: Prentice-Hall, 2005.

[4] M. Nakamura, S. R. Munasinghe, S. Goto and N. Kyura, "Enhanced contour control of SCARA robot under torque saturation constraint," *IEEE/ASME Transactions on Mechatronics*, vol. 5, no. 4, pp. 437-440, Dec. 2000.

[5] M. L. Balter, A. I. Chen, T. J. Maguire and M.L. Yarmush, "The System Design and Evaluation of a 7-DOF Image-Guided Venipuncture Robot," *IEEE Transactions on Robotics*, vol. 31, no. 4, pp. 1044-1053, Aug. 2015.

[6] Z. Zhang, L. Zheng, J. Yu, Y. Li and Z. Yu, "Three Recurrent Neural Networks and Three Numerical Methods for Solving a Repetitive Motion Planning Scheme of Redundant Robot Manipulators," *IEEE/ASME Transactions on Mechatronics*, vol. 22, no. 3, pp. 1423-1434, Jun. 2017.

[7] M. Jin, S. H. Kang, P. H. Chang and J. Lee, "Robust Control of Robot Manipulators Using Inclusive and Enhanced Time Delay Control," *IEEE/ASME Transactions on Mechatronics*, vol. 22, no. 5, pp. 2141-2152, Oct. 2017.

[8] F. Cheng, L. Qu and W. Qiao, "Fault Prognosis and Remaining Useful Life Prediction of Wind Turbine Gearboxes Using Current Signal Analysis," *IEEE Transactions on Sustainable Energy*, vol. 9, no. 1, pp. 157-167, Jan. 2018.

[9] G. Wang, R. Yang and J. Xu, "DSP-Based Control of Sensorless IPMSM Drives for Wide-Speed-Range Operation," *IEEE Transactions on Industrial Electronics*, vol. 60, no. 2, pp. 720-727, Feb. 2013.

IEEE/ASME TRANSACTIONS ON MECHATRONICS

[10] P. Mercorelli, "A Motion-Sensorless Control for Intake Valves in Combustion Engines," *IEEE Transactions on Industrial Electronics*, vol. 64, no. 4, pp. 3402-3412, April 2017.

[11] A. Jena, P. K. Sahu, S. C. Bharat and B. B. Biswal, "Optimal trajectory planning of a 3R SCARA manipulator using geodesic," *IEEE International Conference on Power Electronics, Intelligent Control and Energy Systems (ICPEICES)*, pp. 1-6, July 2016.

[12] C. Gosselin, M. Isaksson, K. Marlow and T. Laliberté, "Workspace and Sensitivity Analysis of a Novel Nonredundant Parallel SCARA Robot Featuring Infinite Tool Rotation," *IEEE Robotics and Automation Letters*, vol. 1, no. 2, pp. 776-783, July 2016.

[13] S. Krupínski, G. Allibert, M. D. Hua and T. Hamel, "An Inertial-Aided Homography-Based Visual Servo Control Approach for (Almost) Fully Actuated Autonomous Underwater Vehicles," *IEEE Transactions on Robotics,* vol. 33, no. 5, pp. 1041-1060, Oct. 2017.

[14] A. N. Montanari and E. de Souza Oliveira, "A Novel Analog Multisensor Design Based on Fuzzy Logic: A Magnetic Encoder Application," *IEEE Sensors Journal,* vol. 17, no. 21, pp. 7096-7104, Nov. 2017.

[15] K. Tobita, T. Ohira, M. Kajitani, C. Kanamori, M. Shimojo and Aiguo Ming, "A rotary encoder based on magneto-optical storage," *IEEE/ASME Transactions on Mechatronics*, vol. 10, no. 1, pp. 87-97, Feb. 2005.

[16] P. Voglewede, A. H. C. Smith and A. Monti, "Dynamic Performance of a SCARA Robot Manipulator With Uncertainty Using Polynomial Chaos Theory," *IEEE Transactions on Robotics*, vol. 25, no. 1, pp. 206-210, Feb. 2009.

[17] F. G. Rossomando and C. M. Soria, "Adaptive Neural Sliding Mode Control in Discrete Time for a SCARA robot arm," *IEEE Latin America Transactions*, vol. 14, no. 6, pp. 2556-2564, Jun. 2016.

[18] H. W. Chow, Norbert C. Cheung, W. Jin, "A Low-Cost Submicrolinear Incremental encoder Based on 3×3 Fiber-Optic Directional Coupler," *IEEE Transactions on Instrumentation and Measurement,* vol. 59, no. 6, pp. 1624-1633, Jun. 2010.

[19] Z. Yang and X. Wang and P. K. Wong, "Single and Simultaneous Fault Diagnosis With Application to a Multistage Gearbox: A Versatile Dual-ELM Network Approach," *IEEE Transactions on Industrial Informatics*, vol. 14, no. 12, pp. 5245-5255, Dec. 2018.

[20] J. Wang and F. Cheng and W. Qiao and L. Qu, "Multiscale Filtering Reconstruction for Wind Turbine Gearbox Fault Diagnosis Under Varying-Speed and Noisy Conditions," *IEEE Transactions on Industrial Electronics*, vol. 65, no. 5, pp. 4268-4278, May 2018.

[21] M. Zhao, M. Kang, B. Tang and M. Pecht, "Deep Residual Networks With Dynamically Weighted Wavelet Coefficients for Fault Diagnosis of Planetary Gearboxes," *IEEE Transactions on Industrial Electronics*, vol. 65, no. 5, pp. 4290-4300, May 2018.

[22] Y. Huang, "Research on Reducer Operation Status Monitoring and Fault Diagnosis System," M.S. thesis, Dept. Dalian Jiaotong University, Dalian, China, 2015.

[23] D. Xiao, "Research on Transmission Error of RV Reducer," M.S. thesis, Dept. Beijing University of Technology, Beijing, China, 2018.

[24] E. Brassitos, N. Jalili, "Dynamic Model Development and Characterization of Gear Bearing Transmission Systems: Theory and Experiments," *IEEE/ASME Transactions on Mechatronics*, vol. 24, no. 4, pp. 1651-1661, Aug. 2019.

[25] J. Park, J. M. Ha, H. Oh, B. D. Youn, J. Choi and N. H. Kim, "Model-Based Fault Diagnosis of a Planetary Gear: A Novel Approach Using Transmission Error," *IEEE Transactions on Reliability*, vol. 65, no. 4, pp. 1830-1841, Dec. 2016.

Bo Tang received the B.S. degree in mechanical and electrical engineering from Chongqing University of Science and Technology, Chongqing, China, in 2019. He is currently pursuing a master degree in mechanical and electrical engineering from Zhejiang Sci-Tech University, Zhejiang, China.
His research interests include design of electrical motor drives, and control of permanent magnet synchronous motor.

Yaxiong Wu received the B.S. degree from Lanzhou University of Technology, Lanzhou, China, in 2018. He is currently pursuing a master degree in mechanical engineering from Zhejiang Sci-Tech University, Hangzhou, China.
His research interests include robotic motor drives, high-speed, high-precision servo drives for synchronous motors and permanent magnet AC servo systems.

Kaiyuan Lu (M'11) received the B.S. and M.S. degrees from Zhejiang University, Zhejiang, China, in 1997 and 2000 respectively, and the Ph.D. degree from Aalborg University, Denmark, in 2005, all in electrical engineering.
In 2005, he became an Assistance Professor with the Department of Energy Technology, Aalborg University, where he has been an Associate Professor since 2008. His research interests include the design of permanent magnet machines, finite element method analysis, and control of permanent magnet machines.

Dong Wang (S'13-M'16) received the B.S. degree from Zhejiang University, Zhejiang, China, in 2004, and the M.S. and Ph.D. degrees from Aalborg University, Denmark, in 2006 and 2016, respectively, all in electrical engineering.
From 2006 to 2012, he was with Grundfos R&D China, Suzhou, China, as a Senior Motor Engineer, working on the design and analysis of the permanent magnet machine and devices. From 2016 to 2017, he was a Postdoc Researcher with the Department of Energy Technology, Aalborg University, where he has been an Assistant Professor since 2017. His research interests include design and control of synchronous reluctance and permanent magnet machines.

Wenqi Lu received the B.S.degree from Zhejiang Ocean University, Zhejiang, China, in 2005, and the Ph.D.degree from Nanjing University of Aeronautics and Astronautics, Nanjing, China, in 2011.
From 2014 to 2017, he was a Post-Doctoral Researcher with the Department of Electrical Engineering, Zhejiang University. From 2017 to 2018, he was a Guest Researcher with the Department of Energy Technology, Aalborg University. He is currently an Associate Professor with the Faculty of Mechanical Engineering and Automation, Zhejiang Sci-Tech University. His current research interests include the control of electric machines and mechatronic system and its application in robot and intelligent manufacturing equipment.

XiuFeng Wang received the B.S. degree from Wuhan University of Technology, Wuhan, China in 2000, and the M.S. degrees from Wuhan University of Technology, Wuhan, China in 2005.
From 2000 to 2002, he worked in YTO Group Corporation, Luoyang, China, as a Senior Mechanical Engineer, principally on mold design of the precision casting. From 2005 to 2015, he worked in Zhejiang Branch of Institute of Computing Technology Chinese Academy of Science, as the Taizhou Branch's Director and Zhejiang Branch's assistant director, principally on R&D and transformation of scientific and technological achievements. He worked in Hangzhou Qixing Robot Technology CO.LTD since 2015 as CEO, His research interests include design and control industry robot.